AN EXPERIMENTAL STUDY ON THE EFFECT OF STRUCTURE OF HOT SIDE AND COOL SIDE HEATSINK TO PERFORMANCES OF THERMOELECTRIC GENERATOR UNIT USING HEAT SOURCE FROM EXHAUST GAS OF MOTORCYCLE

Hong Duc Thong[1], Vo Tan Phat[1], Tran Quang Khoi[1], Mai Van Tinh[1], Nghiem Phan Thien Quan[1], Pham Quang Minh[1], Do Minh Dung[1], Tran Trong Khiem[2]
[1] Ho Chi Minh City University of Technology, Vietnam
[2] Ho Chi Minh City University of Agriculture and Forestry, Vietnam

Received 01/11/2018, Peer-reviewed 22/11/2018, Accepted for publication 11/12/2018

ABSTRACT

This study investigates the effect of Hot Side Heatsink (HSH) and Cool Side Heatsink (CSH) on the temperature of the hot and cool side and output power of the Thermoelectric Generator Unit (TGU). The structure of the HSH and the CSH is designed and manufactured based on the results of calculating the heat transfer through the TGU with Matlab Script and simulation with ANSYS software. The TGU consists of 08 TEP1-142T300 ThermoElectric Generator (TEG) modules connected in series and use heat from the exhaust gas of the Suzuki Sapphire 125 engine was conducted in the range of speed from 20km/h to 60km/h. The results show that increasing the number of fins of HSH and CSH leads to the increase of output power of the TGU. The output powers between test cases are significantly different when the vehicle speed increases. The output power of the TGU can reach about 1.1W at 20km/h, and 14.1W at 60km/h. The temperature of the hot side and cool side of the TGU obtained from the calculation, simulation and experiment are very different. This difference is due to the quality of the material, the surface roughness and the dust, dirty of the HSH and CSH cause significant differences between the practical and theoretical. This study has important implications, as a basis for (1) calculating and estimating the actual thermal conductivity of the material of HSH and CSH; and (2) optimizing calculation the structure of the HSH and CSH to enhance the capacity and durability of the TGU.

Keywords: *Thermoelectric generator unit; hot side heatsink; cool side heatsink; temperature; output power; exhaust gas.*

1. INTRODUCTION

Today, fuel crises, environment pollution and energy security are all important issues for every country in the world, from developed countries to developing countries. This has promoted researches about the efficient use of energy as well as the reuse of energy resources that are being wasted. According to a study by Stabler [1], the heat energy in the exhaust gas of internal combustion engines accounted for 35 to 40% of the energy generated during combustion. In fact, this form of energy is wasted into the environment. With the development of the TEG modules, the possibility of exploiting this heat source becomes more feasible. This issue has attracted the attention of researchers and many scientific works have been done on the application of TEG modules on a variety of subjects such as internal combustion engine [2-6], vehicle [7-10] and geothermal [11].

The above studies are mainly based on the difference in temperature (ΔT) between the hot side and cool side of TGU to produce electricity without considering the effect of the hot side temperature (T_h) and the cool side temperature (T_c) to the output power of the TGU. Meanwhile, the fin structure and

especially the heat transfer area of the HSH and CSH greatly affect the output power of the TGU.

In this study, the authors investigated the change of the hot side temperature (T_h) and the cool side temperature (T_c) of the TGU consisting of 08 TEP1-142T300 TEG modules connected in series by changing the structure of the HSH and the CSH. This system was put on Suzuki Sapphire 125 motorcycle, and experimented at different speed ranges from 20km/h to 60km/h. The structure of the HSH and the CSH is designed and manufactured for this experimental study is based on the calculation results of heat transfer by the MATLAB model developed and compared by the authors alongside with simulation results by ANSYS software.

The purpose of this study is to show the influence of heat transfer, heat recovery and heat dissipation on the hot side temperature, cool side temperature, temperature difference, and the output power of the TGU. The results have an important role as a basis for optimizing the structure, capacity, and durability of the TGU.

2. BASIS OF THEORY

2.1. Heat transfer

2.1.1. Calculating the convection heat transfer coefficient

In this study, the authors used the flat plate model to calculate the convection heat transfer coefficient.

The Reynolds number is defined as:

$$\mathrm{Re}_f = \frac{\omega.l}{\nu} \quad (1)$$

Where: ω (m/s) is the average fluid speed, l (m) is the characteristic length and ν (m^2/s) is the kinematic viscosity coefficient.

To calculate the convection heat transfer coefficient, the Nusselt number Nu_f is required:

$$\text{If } \mathrm{Re}_f \geq 10^5: \quad Nu_f = 0.032\,\mathrm{Re}_f^{0.8} \quad (2)$$

$$\text{If } \mathrm{Re}_f < 10^5: \quad Nu_f = 0.59\,\mathrm{Re}_f^{0.55} \quad (3)$$

The convection heat transfer coefficient α ($W/m^2.K$) is calculated using the formula:

$$\alpha = \frac{Nu_f.\lambda}{l} \quad (4)$$

Where: λ ($W/m.^0C$) is the thermal conductivity of the fluid.

2.1.2. Calculating the heat rate transferring through the TGU

Using the Newton formula, the heat rate by convection Q (W) is:

$$Q = \alpha.F(T_w - T_f) \quad (5)$$

Where: F (m^2) is the heat transfer area, T_w (^0C) is the average temperature of heat transfer surface and T_f (^0C) is the average temperature of fluid.

The heat rate by conduction Q (W) is calculated using the formula:

$$Q = \frac{\lambda}{\delta} F(T_{W1} - T_{W2}) \quad (6)$$

$$q_x = \frac{Q}{F} \quad (7)$$

Where: δ (m) is the thickness of solid, F (m^2) is the area which is perpendicular to the direction of transfer, T_{W1} (^0C) is the average temperature of hot side of solid, T_{W2} (^0C) is the average temperature of cool side of solid and q_x (W/m^2) is the heat flux.

The heat rate of both conduction and convection Q (W) is calculated using the formula:

$$Q = k(T_{f1} - T_{f2})F \quad (8)$$

Where: k ($W/m^2.K$) is the overall heat transfer coefficient, T_{f1} (^0C) is the average temperature of fluid at the hot side of object and T_{f2} (^0C) is the average temperature of fluid at the cool side of object.

2.2. Seebeck effect

Seebeck the effect is the phenomenon of thermal energy is converted directly into electrical energy in a closed circuit consisting

of two metallic conductors has some connections (welds) together, it is called a closed circuit thermocouple. The current is generated by the temperature difference between the two welds and intensity proportional to this difference.

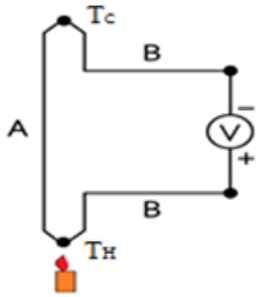

Figure 1. *The closed-circuit thermocouples*

The closed circuit thermocouples are presented in Figure 1, in which A and B are the two different materials; T_H and T_C are the temperature of hot source and cold source, respectively.

The voltage of the electrical current is calculated using the formula:

$$U_S = S(T_h - T_c) = S.\Delta T \quad (9)$$

Where: S (V/K) is Seebeck coefficient, T_h (^{0}C) is temperatures of a hot side, T_c (^{0}C) is temperatures of cool side, ΔT (^{0}C) is temperature difference between hot side and cool side.

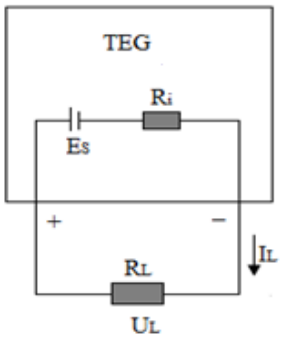

Figure 2. *Mathematical model of TEG modules*

Considering the circuit provides load (Figure 2) of TEG, we have the following equation:

$$U_S = E_S = S.\Delta T \quad (10)$$

$$I_L = \frac{E_S}{R_i + R_L} = \frac{S.\Delta T}{R_i + R_L} \quad (11)$$

$$U_L = I_L R_L = E_S - I_L R_i \quad (12)$$

$$Q_{in} = k_T.\Delta T + S.T_h.I_L - 0{,}5.R_i.I_L^2 \quad (13)$$

$$Q_{out} = k_T.\Delta T + S.T_c.I_L + 0{,}5.R_i.I_L^2 \quad (14)$$

$$k_T = N(k_n + k_p)G \quad (15)$$

$$P_L = I_L.U_L = Q_{in} - Q_{out} = S.I_L.\Delta T - R_i I_L^2 \quad (16)$$

Where: E_S (V) is the electromotive force of TEG; U_S (V) is the voltage generated by the Seebeck effect; S (V/K) is Seebeck coefficient; R_i (Ω) is the resistance of the TEG; R_L (Ω) is the load resistor; T_h (^{0}C) is the temperature of hot side; T_c (^{0}C) is the temperature of cool side; ΔT (^{0}C) is the temperature difference between hot side and cool side; k_T (W/K) is the thermal conductance of TEG; N is the number of thermocouples; k_n (W/m.K) and k_p (W/m.K) are the thermal conductivities of material n and p, respectively; G (m) is the geometry factor (G = area/length); P_L (W) is the output power with load, Q_{in} (W) is the heat input, Q_{out} (W) is the heat output, I_L (A) is the amperage, U_L (V) is the voltage.

3. RESEARCH MODEL

3.1. Thermoelectric Generator Unit-TGU

The TGU's structure with exhaust pipe is shown in Figure 3, which includes: exhaust pipe (7) designed for Suzuki Sapphire 125cc motorbike; the HSH (5); 08 TEP1-142T300 TEG modules connected in series (4); the CSH (1). In addition, the system has other components such as screws (3) and gasket (6) to connect the HSH (5) to the exhaust pipe (7); the nuts (2), the threaded rods (8), the washers (9) and the springs (10) for pressing the CSH (1), TEG modules (4) and the HSH (5) together. Between the CSH (1) and the TEG modules (4), as well as between the

TEG modules (4) and the HSH (5), there is a layer of thermal compound.

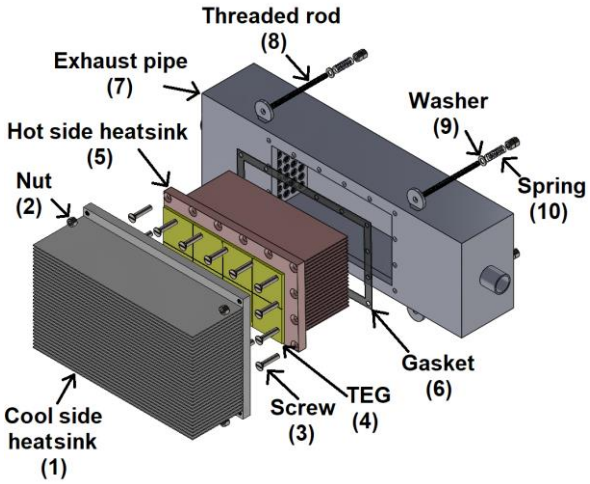

Figure 3. *Structure of the TGU with the exhaust pipe*

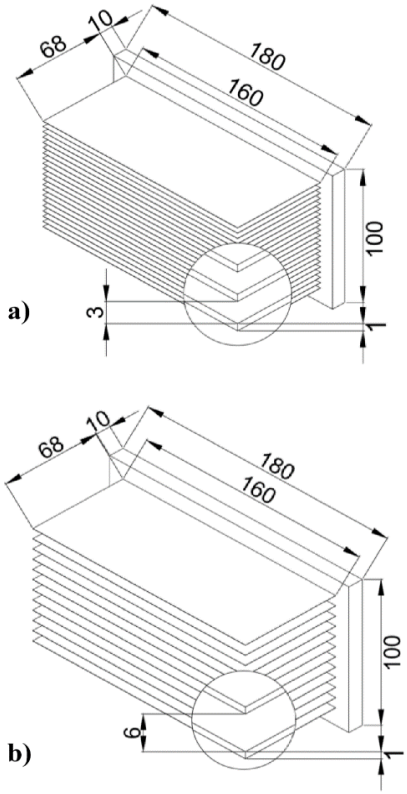

Figure 4. *The dimension of HSH: a) 21 fins; b) 12 fins*

The TEP1-142T300 modules are manufactured by Shenzhen Dowell - Chip Electronics Co., China. Each module sized 40mm x 40mm x 3.4mm, which has the operating temperature range from -40^{0}C to 300^{0}C. In this study, two aluminum HSHs and two aluminum CSHs are designed based on the results of the thermal calculation process on MATLAB Script and simulation on ANSYS software. These heatsinks are used to study the effect of their structure on the temperature at both sides of the TGU and the output power of the TGU. One HSH has 12 fins and another has 21 fins; one CSH has 31 fins and another has 11 fins. The structure of the HSH and CSH are shown in Figures 4 and 5.

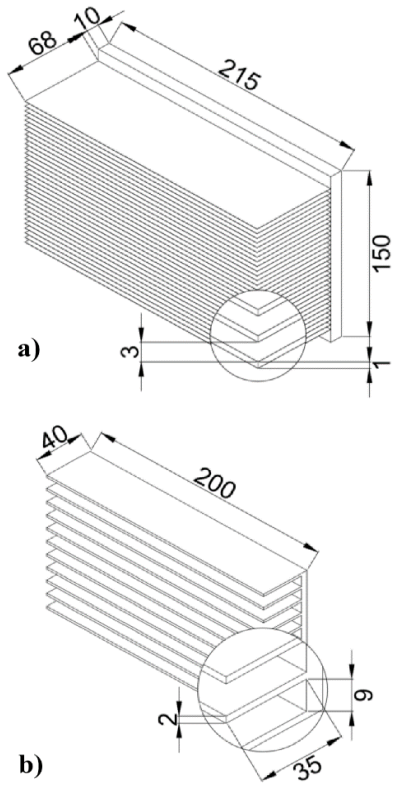

Figure 5. *The dimension of CSH: a) 31 fins; b) 11 fins*

3.2. Calculating the heat transfer

The simulating and calculating process are carried out in three cases with the difference in heatsinks' fin quantity. Case (I): 21 fins of the HSH and 31 fins of the CSH; case (II): 21 fins of the HSH and 11 fins of the CSH and case (III): 12 fins of the HSH and 31 fins of the CSH. The simulating cases are shown in Table 1.

Table 1. *Simulating cases*

Cases	Quantity of fins of the HSH	Quantity of fins of the CSH
(I)	21	31
(II)	21	11
(III)	12	31

3.2.1. Heat transfer calculating model in MATLAB Script

The heat transfer of the TGU was calculated basing on the heat transfer theory with the support of MATLAB Script [12] as shown in Figure 6 with the following hypotheses:

- The heat rate inside of TGU is balanced during the calculating process.
- Disregard the effect of convection heat transfer at the foundation of heatsinks.
- Fin efficiency is considered 100%.

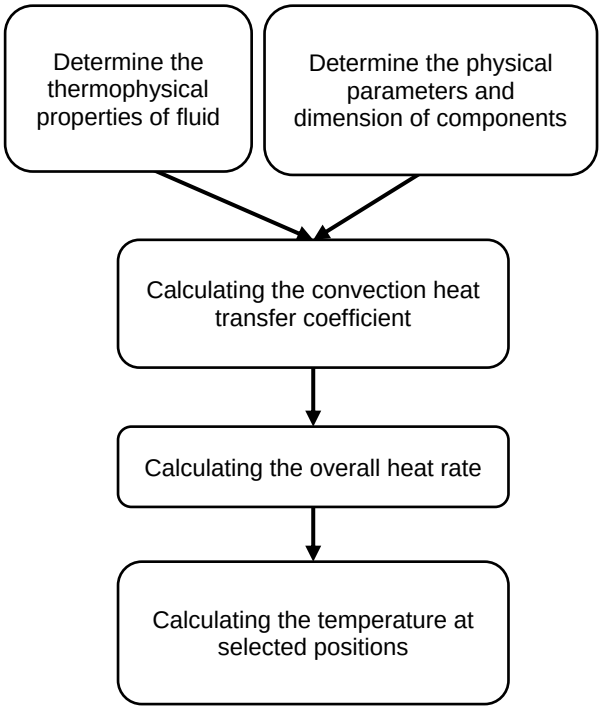

Figure 6. *The heat transfer calculating process of the TGU*

3.2.2. Simulating the heat transfer in ANSYS Software

To validate the accuracy of the MATLAB calculating model, the heat transfer of TGU is simulated using ANSYS software [13]. The simulating process is shown in Figure 7.

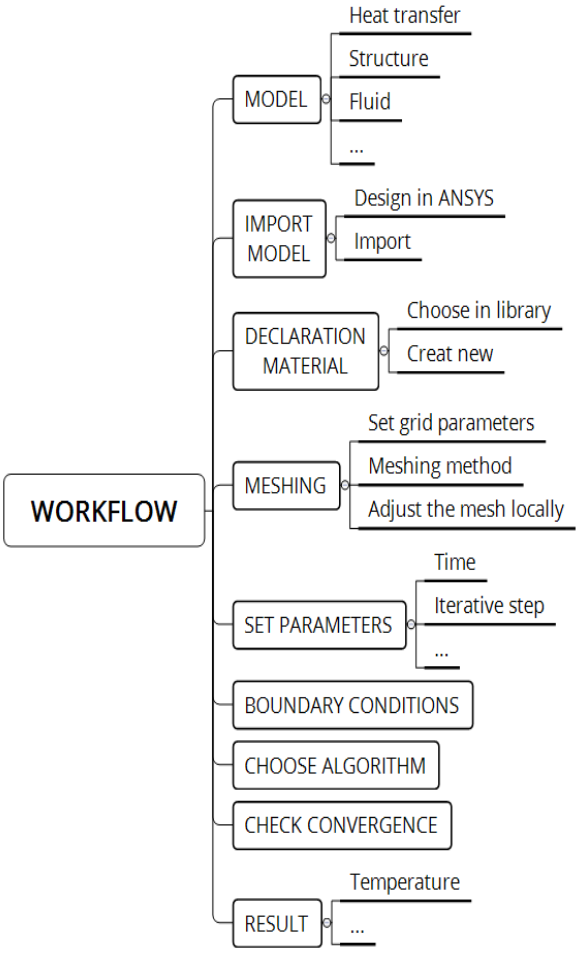

Figure 7. *The heat transfer simulating the process of the TGU*

ANSYS Fluent solves the energy equation in the following form:

$$\frac{\partial}{\partial t}(\rho E)+\nabla.\left(\vec{v}.(\rho E+p)\right)= \nabla.\left(k_{eff}\nabla T-\sum_j h_j\overrightarrow{J_j}+\left(\overline{\overline{\tau_{eff}}}.\vec{v}\right)\right)+S_h \quad (17)$$

Energy equation in solid regions is:

$$\frac{\partial}{\partial t}(\rho h)+\nabla.\left(\vec{v}\rho h\right)=\nabla.(k\nabla T)+S_h \quad (18)$$

Where: ρ is density, v is velocity, p is pressure, k_{eff} is the effective conductivity, T is temperature, J_j is the diffusion flux of

species, $\overline{\overline{\tau_{eff}}}$ is vicious, k is conductivity, S_h includes volumetric heat source that you defined but not the heat sources generated by finite - source volumetric or surface reactions since species formation enthalpy is already included in the total enthalpy calculation. The first three terms on the right - hand side represents energy transfer due to conduction, species diffusion, and viscous dissipation, respectively. And:

$$h = \int_{T_{ref}}^{T} C_p dT \text{ : enthalpy} \quad (19)$$

$$h_j = \int_{T_{ref}}^{T} C_{p,j} dT \text{ : enthalpy of species j} \quad (20)$$

(C_p : the specific heat capacity)

$$E = h - \frac{p}{\rho} + \frac{v^2}{2} \quad (21)$$

($h = \sum_j Y_j h_j$, Y_j : the mass fraction of species j)

The boundary condition includes parameters: Specification of material (density, C_p, thermal conductivity), energy source, heat flux, heat transfer coefficient, free steam temperature, inside and outside pressure of exhaust pipe.

MultiZone is meshing method which is used for all parts of the model, and this model was evaluated by the skewness standard. Skewness mesh metrics are shown in Table 2 [13] and the meshing results of cases are shown in Table 3.

Table 2. *Skewness mesh metrics*

Evaluation	**Excellent**	**Very good**
Skewness	0 – 0.25	0.25 – 0.50
Evalution	**Good**	**Acceptable**
Skewness	0.50 – 0.80	0.80 – 0.94
Evaluation	**Bad**	**Unacceptable**
Skewness	0.95 – 0.97	0.98 – 1.00

Table 3. *Meshing results of simulation cases*

Case	**Nodes**	**Elements**	**Skewness average**
(I)	2567620	451736	0.11093
(II)	2643066	452207	0.12116
(III)	2282240	445195	0.15692

Table 4. *Input parameters*

Parameters of materials	**Heatsink (Aluminum)**		**TEG module**
Density (kg/m^3)	2770		5860
Specific capacity (J/kg.K)	925		157.35
Thermal conductivity (W/m.K)	148		15.10^{-3}
Input parameters according to vehicle's speed	**25 km/h**	**40 km/h**	**60 km/h**
Exhaust gas flow rate ($.10^{-3}$ m^3/s)	3.75	4.68	6.25
Average the temperature of exhaust gas in the exhaust pipe (^{0}C)	100	125	246
Speed of air flowing through the CSH (km/h)	25	40	60
Initial temperature of the CSH (^{0}C)	30		
Initial temperature of TEG modules (^{0}C)	30		
Ambient temperature (^{0}C)	30		
Inside and outside the pressure of exhaust pipe (Pa)	101325		

3.2.3. Parameters and conditions in heat transfer simulating and calculating process

The simulating and calculating process are carried out in three cases as mentioned above. In each case, the speeds of vehicle, which are initially chosen, are 25km/h, 40km/h and 60km/h. The input parameters are shown in Table 4.

3.3. Experiment description

Figure 8 shows a diagram of the experimental system. Figure 9 shows the devices mounted on the vehicle. The parameters to be measured in this study include temperature, voltage, current and speed of the vehicle. The temperature is measured by 06 PT100 - WZP50 sensors (diameter D = 4mm and length L = 30mm) at 06 different positions, which are shown in Figure 8: 02 temperature sensors are located at the front and rear of the exhaust pipe to measure the exhaust gas temperature at the inlet and outlet; 02 temperature sensors are located at the 02 different points of the HSH to measure the temperature of the HSH; the other two sensors are located on the CSH, which is symmetrical with two sensors on the HSH, to measure the temperatures of the CSH.

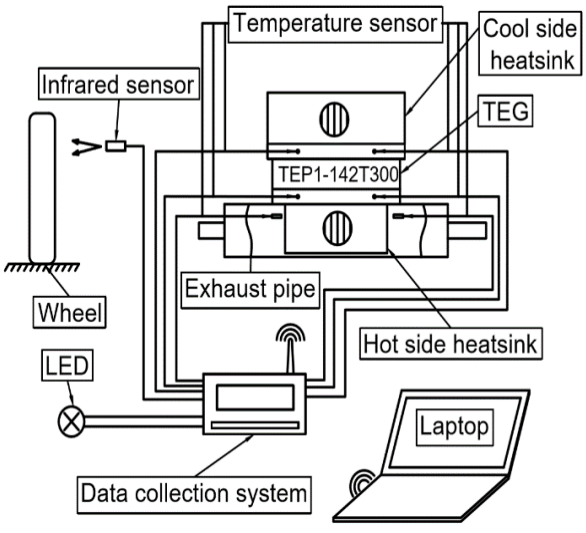

Figure 8. *The diagram of the experimental system*

Figure 9. *The TGU is mounted on the vehicle*

The average temperature difference between the hot and cool side of the TGU was calculated basing on the average temperature of the hot side and cool side of the TGU. Voltage and current are measured by an integrated circuit (power circuit) operating in the ADC method (*Analog-to-digital converter*, the input voltage is converted to the numerical value to represent the magnitude of voltage, the current is calculated based on the initial resistance value and the voltage value). The power generating from TGU is calculated basing on these parameters. The vehicle's speed is measured by the infrared sensor (V1), which is attached on the axle of the front wheel. The microcontroller (Atmega32, manufactured by Atmel Corporation, USA) receives signals from the sensors and power circuits; then transmitted to the laptop via the Bluetooth connection. The parameters of temperature sensors and vehicle speed sensors are shown in Table 5.

Table 5. The parameters of temperature sensors and vehicle speed sensor.

No.	Device	Type	Range	Accuracy
1	Temper-rature sensors	PT100-WZP50 class A	-200^{0}C to 420^{0}C	±0.15^{0}C
2	Vehicle speed sensor	Infrared sensor - V1	Working distance: 2cm to 5cm	-

The change in hot side temperature, cool side temperature and the output power of TGU were studied in three cases with the difference in heatsink fin quantity. Each case is shown in Table 1. In each case, the vehicle's speed ranges from 20km/h to 60km/h.

4. RESULTS AND DISCUSSION

4.1. Calculation and simulation results of heat transfer process

Figure 10-12 shows variation in hot side temperature, cool side temperature and the temperature difference between hot and cool side according to simulated time in three different configurations of HSH and CSH correspond to the vehicle speed at 25km/h, 40km/h, and 60km/h. The results show that the time for the temperature of hot and cool side to become stable in 3 cases at the same speed is almost the same. However, in the same case, the time for temperature of hot and cool side to reach steady state increases as the speed of the vehicle increases; it would take about 400 seconds at 25km/h, about 440 seconds at 40km/h and about 480 seconds at 60km/h for hot and cool side to become stable.

As the speed of the vehicle increases, the heat generated by the exhaust gas increases too. This makes the heat transfer better, thus reducing the steady-state time required for the temperature of the hot and cool side. In addition, as the speed increases, the convection effect increases lead to the amount of heat transferred to the environment increases, thus increasing the steady-state time required for the temperature of the hot and cool side of TGU. The simulated results show that the effect of convection heat transfer on cool side on the steady-state time required is superior to the effect of increased exhaust gas heat due to increasing vehicle's speed.

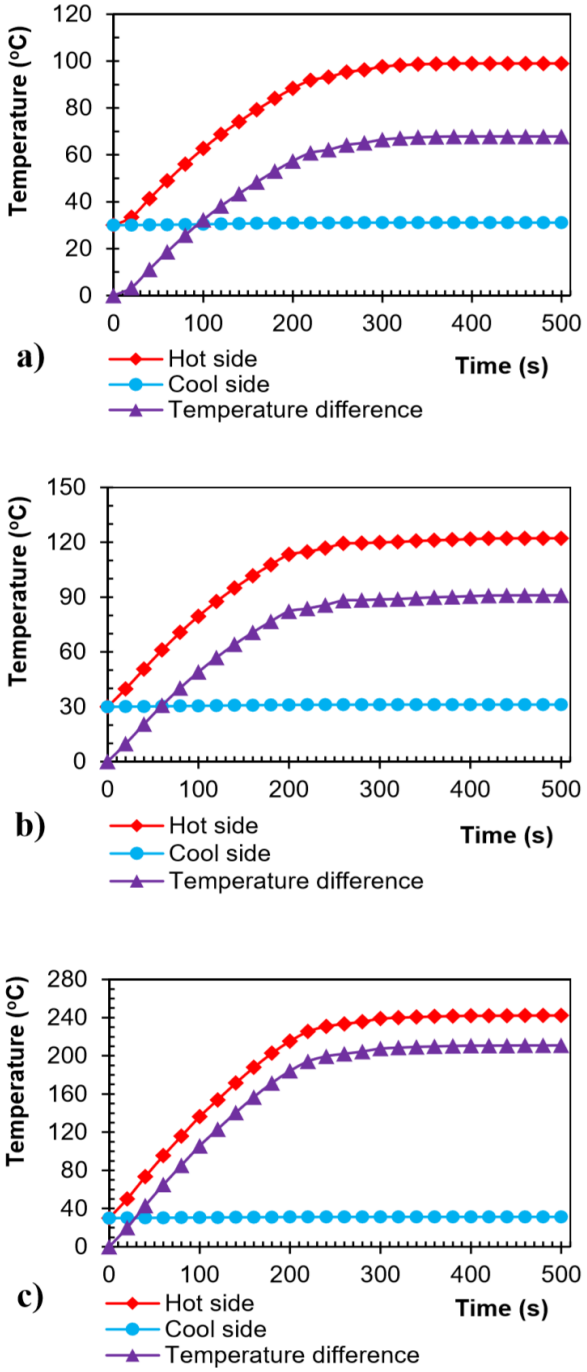

Figure 10. *Characteristics of hot side temperature, cool side temperature, and temperature difference over simulation time in case I (21 fins of HSH and 31 fins of CSH): a) at 25km/h; b) at 40km/h; and c) at 60km/h*

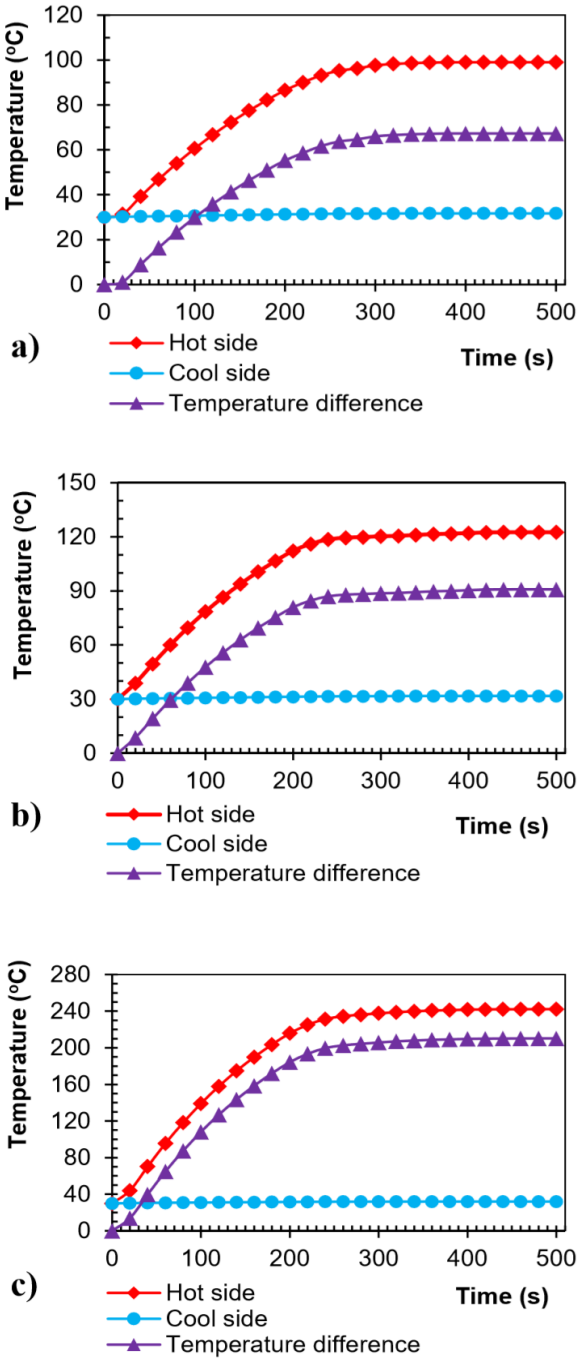

Figure 11. *Characteristics of hot side temperature, cool side temperature, and temperature difference over simulation time in case II (21 fins of HSH and 11 fins of CSH): a) at 25km/h; b) at 40km/h; and c) at 60km/h*

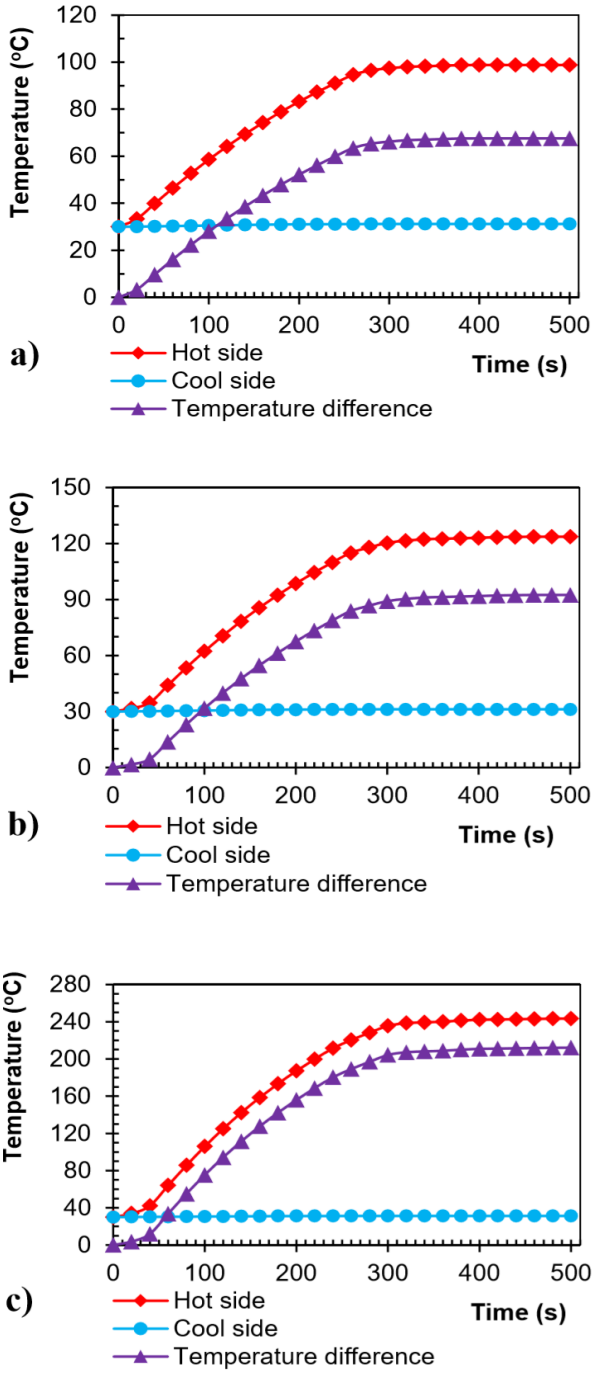

Figure 12. *Characteristics of hot side temperature, cool side temperature, and temperature difference over simulation time in case III (12 fins of HSH and 31 fins of CSH): a) at 25km/h; b) at 40km/h; and c) at 60km/h*

Table 6 shows the results of calculations and simulation of hot side and cool side temperature in three cases with vehicle speed at 25km/h, 40km/h, and 60km/h. The results show that the difference between the calculated and simulated values is about 1^0C to 2^0C and the deviation increases as the speed of the vehicle increases. The difference between the MATLAB calculation and ANSYS simulation is due to: (i) the MATLAB model ignores the convection heat transfer of the foundation of heatsinks; (ii)

another problem that could lead to difference is that in the MATLAB model, the heat loss due to the heat transfer to the environment of the TGU is not taken into account, whereas the ANSYS simulation can account for the amount this heat.

Table 6. *Temperature results of cool and hot side of the TGU in calculation and simulation: T_h - Hot side temperature; T_c - Cool side temperature*

Case I (21 fins of HSH and 31 fins of CSH)			
Temperature		**Calculation**	**Simulation**
25 km/h	T_h (^{0}C)	99.20	99.00
	T_c (^{0}C)	30.10	31.11
40 km/h	T_h (^{0}C)	124.04	122.16
	T_c (^{0}C)	30.10	31.18
60 km/h	T_h (^{0}C)	244.07	242.19
	T_c (^{0}C)	30.17	31.27
Case II (21 fins of HSH and 11 fins of CSH)			
Temperature		**Calculation**	**Simulation**
25 km/h	T_h (^{0}C)	99.20	99.00
	T_c (^{0}C)	30.52	31.70
40 km/h	T_h (^{0}C)	124.04	122.56
	T_c (^{0}C)	30.53	31.74
60 km/h	T_h (^{0}C)	244.08	242.21
	T_c (^{0}C)	30.76	31.95
Case III (12 fins of HSH and 31 fins of CSH)			
Temperature		**Calculation**	**Simulation**
25 km/h	T_h (^{0}C)	98.63	98.80
	T_c (^{0}C)	30.10	31.20
40 km/h	T_h (^{0}C)	123.34	123.64
	T_c (^{0}C)	30.10	31.20
60 km/h	T_h (^{0}C)	242.68	243.40
	T_c (^{0}C)	30.17	31.27

4.2. Experimental results

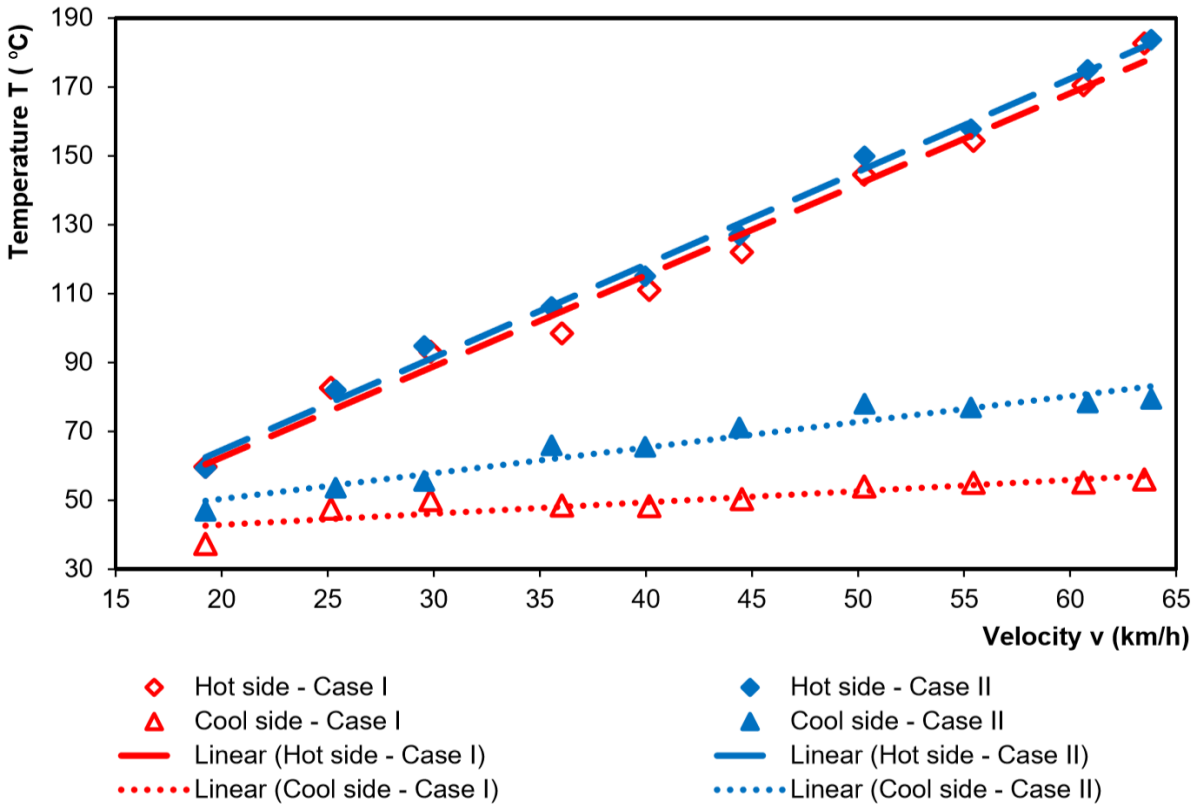

Figure 13. *Characteristics of hot side temperature and cool side temperature correspond to vehicle speed in case I (21 fins of HSH and 31 fins of CSH) and case II (21 fins of HSH and 11 fins of CSH)*

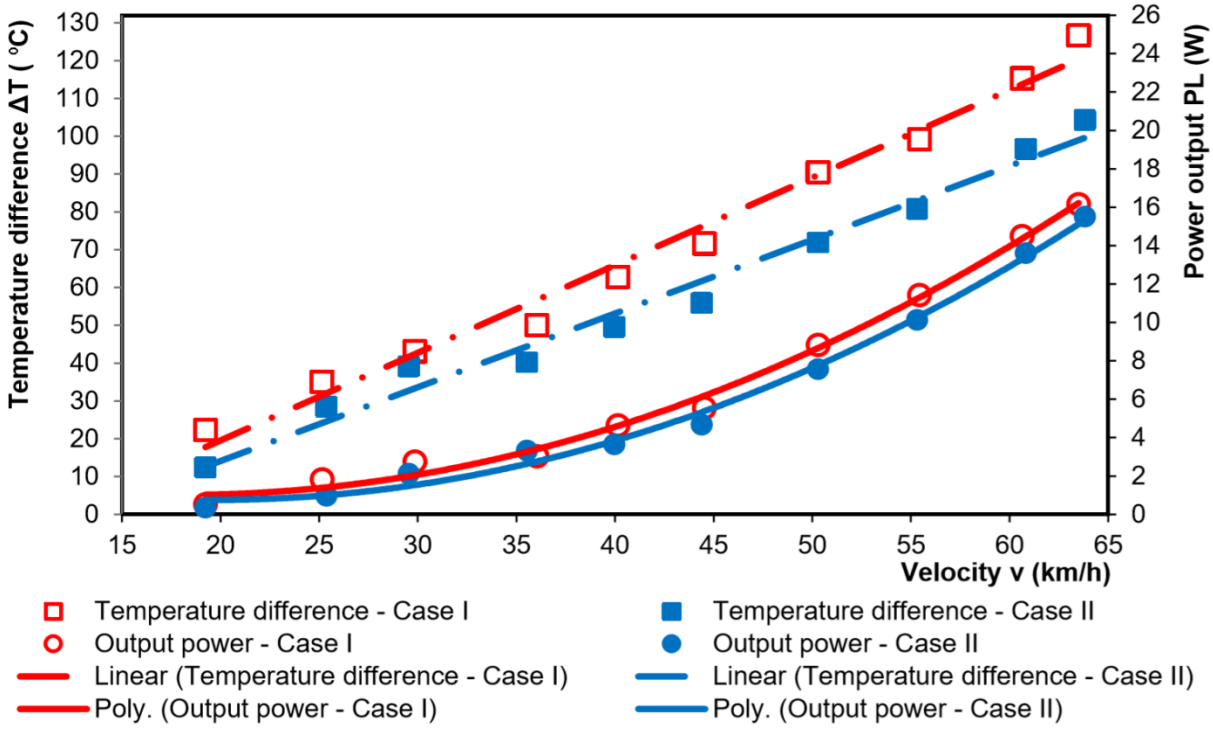

Figure 14. *Characteristics of output power and temperature difference between the hot and cool side correspond to vehicle speed in case I (21 fins of HSH and 31 fins of CSH) and case II (21 fins of HSH and 11 fins of CSH)*

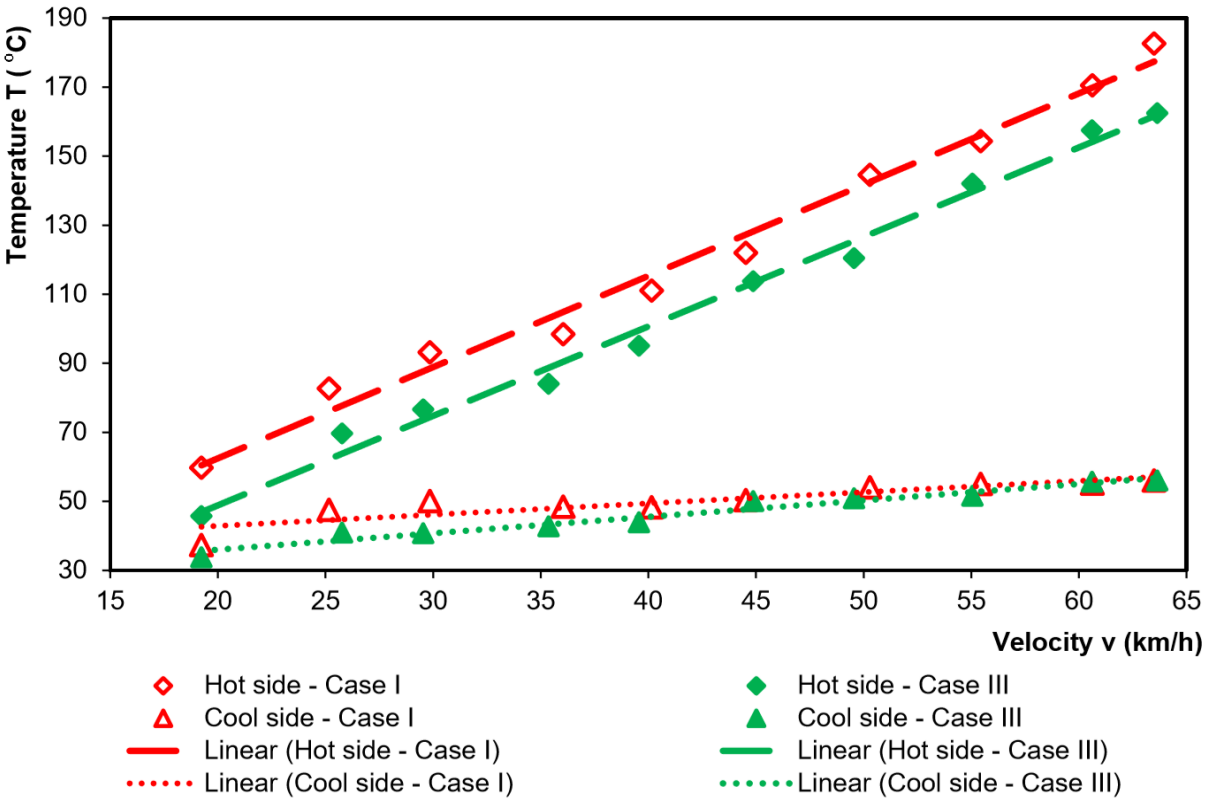

Figure 15. *Characteristics of hot side temperature and cool side temperature correspond to vehicle speed in case I (21 fins of HSH and 31 fins of CSH) and case III (12 fins of HSH and 31 fins of CSH)*

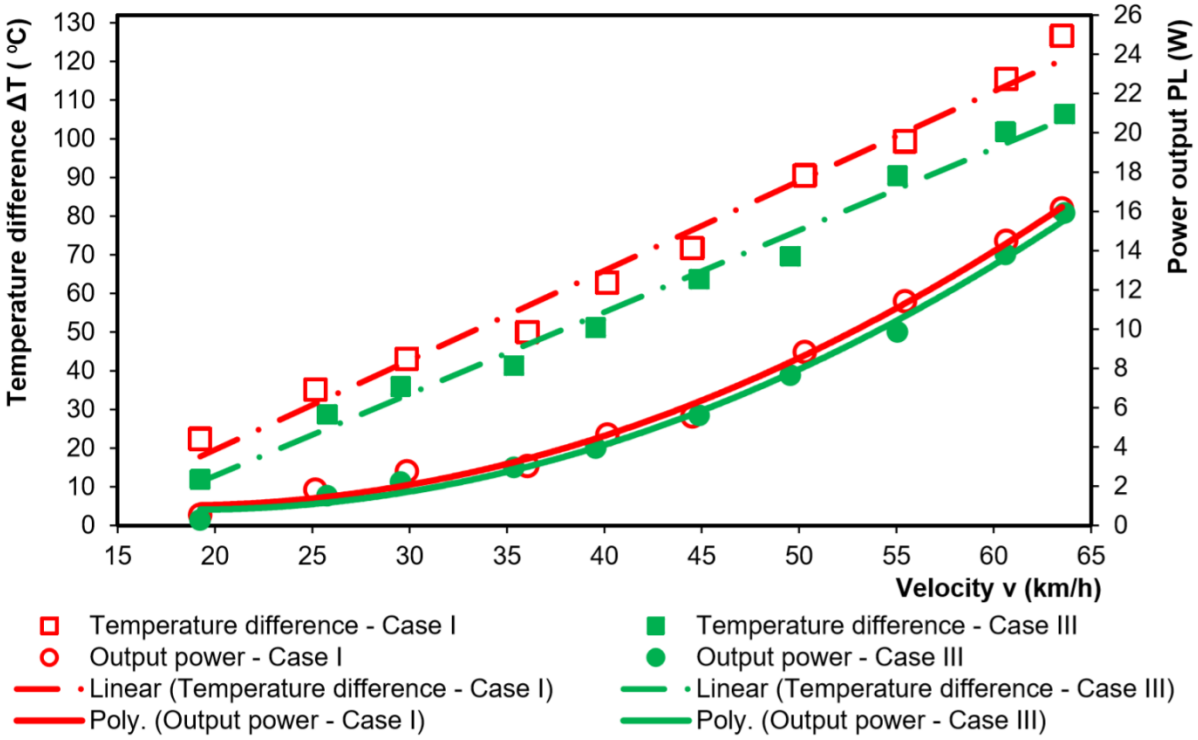

Figure 16. *Characteristics of output power and temperature difference between hot and cool side correspond to vehicle speed in case I (21 fins of HSH and 31 fins of CSH) and case III (12 fins of HSH and 31 fins of CSH)*

Figures 13 and 14 compare the hot side temperature, cool side temperature, the temperature difference between the hot and cool side, and the output power of cases (I) and (II).

Experiment results in Figure 13 show that the hot side temperature in cases (I) and (II) does not seem to change. Meanwhile, the cool side temperature of case (I) is significantly greater than that of case (II). The difference in cool side temperature of these two cases increase as the vehicle's speed increases and reaches 7.5^0C when the speed of the vehicle reaches 20km/h. At the speed of 60km/h, the temperature difference is about 24.3^0C.

Figure 14 shows that the output power and the temperature difference between the hot and cool side of case (I) are higher than case (II) and the difference in these characteristic curves increases with the speed of the vehicle. At 20km/h, the output power of case (I) reaches 1.1W and output power of case (II) reaches 0.8W. So, the output power of case (I) is greater than the case (II) 0.3W. At 60km/h the output power of case (I) reaches 14.1W and the output power of case (II) reaches 13.0W. So, the output power of case (I) greater than the case (II) of 1.1W.

This is explained by the fact that case (I) has more CSH fins than case (II) lead to a lower cool side temperature in case (I). As the speed of the vehicle increases, the heat transfer of the CSH due to convection increases significantly. That leads to the temperature difference between two cool side temperatures of the two cases, as a consequence, increasing.

Figures 15 and 16 compare the hot side temperature, cool side temperature, the temperature difference between the hot and cool side, and the output power of cases (I) and (III).

Figure 15 shows that the hot side temperature of case (I) is always higher than case (III) about 13.6^0C to 15.7^0C in the

experiment speed range of the vehicle. This is due to HSH of (I) has more fins than case (III). The temperature of the cool side of case (I) is higher than of case (III) about 6.9^0C at 20km/h, which is explained by the amount of heat collected from the HSH and transmitted to the CSH in case (I) more than in case (III). However, as the speed of the vehicle increases, the convection heat transfer of the CSH with the environment takes place and the cool side temperature difference between two cases are negligible, about 1^0C at 60km/h.

Figure 16 shows that the output power and the temperature difference between the hot side and cool side of case (I) is higher than case (III). As the speed of the vehicle increases, the difference in output power and the temperature difference between the hot and cool side of the two cases increases. At 20km/h, the output power of case (III) reaches 0.8W, lower than case (I) about 0.3W; and at 60km/h the output power of case (III) reached 13.2W, lower case (I) 0.9W.

It is noteworthy that the hot side temperature and the cool side temperature of the TGU have a very large difference between the results of the empirical survey and the calculation and simulation. The hot side temperature at 60km/h from the simulation and calculation is about 242^0C to 244^0C, while the experimental value is about 153^0C to 172^0C. Cool side temperature at 60km/h from simulation and calculation is about 30^0C to 32^0C, while the experimental value is about 55^0C to 80^0C. The difference between empirical and computed values is explained by the following reasons:

- The thermal conductivity of the HSH material and the CSH material used for calculation and simulation is chosen as an aluminum alloy (92% Aluminum, 8% Magnesium), in fact the real material quality of these components may be poorer, resulting in better calculation and simulation of heat recovery ability as well as CSH cooling ability than the results of experiments.

- The model used in the calculation, simulation is an ideal model with a surface considered absolute plane so the heat transfer between the exhaust gas and the surface of the HSH's fins is ideal. Meanwhile, the actual HSH's fins have surface roughness and soot caused by the engine during the experiment that sticks to the surface of the fins. These agents reduce the convection heat transfer coefficient between the exhaust gas and the HSH's fins. As a result, the heat absorbed by the HSH in the experiment is lower than in the simulation.

- As well as the HSH, the CSH's fins actually have a surface roughness, which, after a period of use, is dirted. This reduces the convection heat transfer coefficient between the air and the CSH's fins, lead to a much lower heat dissipation to the environment than in simulation.

5. CONCLUSION

This study includes calculating, simulating the temperature of both sides of TGU and conducting experiments on the TGU in practical conditions. The work results in the conclusion as follows:

- The structure of the HSH and the CSH considerably affected the temperature at both sides of the TGU and the output power generated from the TGU. The TGU will generate more power when increasing the number of fins of the HSH and the CSH.

- The output power difference between experiment cases increases when increasing the speed of the vehicle. This result proved that the effect of the convection heat transfer of the CSH is considerable at high speed.

- In case (I) (21 fins of HSH and 31 fins of CSH), the TGU generated 1.1W at 20km/h and 14.1W at 60km/h.

- The quality of material, the surface roughness and the accumulation of dirt on heatsinks lead to the differences in temperature at both sides of the TGU between calculating, simulating and experimental processes.

This study motivates issues about the characteristic and optimizing the structure of TGU:

- Calculating the thermal conductivity of material used to manufacture heatsink based on the temperature at the hot side and cool side from the experimental process.
- Calculating to optimize the structure of heatsink in order to improve the output power from TGU, also prolong the longevity of it.

ACKNOWLEDGMENT

This research is funded by Ho Chi Minh City University of Technology (Viet Nam) under grant number T-KTGT-2017-62.

REFERENCES

[1] F. Stabler, Automotive TGU Design Issues, *DOE Thermoelectric Applications Workshop*, January 2011.
[2] J. C. Bass, N. C. Elsner and F. A. Leavitt, Performance of the 1 kW TGU for Diesel Engines, *Proceedings of the 13th international conference on thermoelectrics*, New York 1995.
[3] P. Aranguren, D. Astrain, A. Rodríguez and A. Martínez, Experimental investigation of the applicability of a TGU to recover waste heat from a combustion chamber, *Applied Energy*, 152, pp.121-130, 2015.
[4] T. M. Jeng, S. C. Tzeng, B. J. Yang and Y. C. Li, Design, Manufacture and Performance Test of the TGU System for Waste Heat Recovery of Engine Exhaust, *Inventions*, 1, 2016. doi:10.3390/inventions1010002
[5] C. T. Hsu, G. Y. Huang, H. S. Chu, B. Yu and D. J. Yao, Experiments and simulatons on low-temperature waste heat harvesting system by thermoelectric power generators, *Applied Energy*, 88, pp.1191-1297, 2011.1
[6] Q. V. Le, *The study on making thermoelectric generator using heat energy from the engine exhaust*, Master Thesis, Ho Chi Minh City University of Technology and Education, 2014.
[7] K. Ikoma, M. Munekiyo, K. Furuya, M. Kabayashi, H. Komatsu and K. Shinohara, TGU for Gasoline Engine Vehicles Using Bi_2Te_3 Modues , *J. Japan Inst. Metals*, 63, pp.1475-1478, 1999.
[8] S. K. Kim, B. C. Won, S. H. Rhi, S. H. Kim, J. H. Yoo and J. C. Jang, Thermoelectric Power Generation System for Future Hybrid Vehicles Using Hot Exhaust Gas, *Journal of ELECTRONIC MATERIALS*, 40, pp.778-783, 2011.
[9] Y. Zhang, M. Cleary, X. Wang, N. Kempf, L. Schoensee, J. Yang, G. Joshi and L. Meda, High-temperature and high-power-density nanostructured TGU for automotive waste heat recovery, *Energy Conversion and Management*, 105, pp.946-950, 2015.
[10] V. H. Nguyen, *Research on the use of waste heat from internal combustion engines to generate electricity*, Master Thesis, Ho Chi Minh City University of Technology, 2016.
[11] C. Liu, P. Chen and K. Li, A 1kW TGU for Low-temperature Geothermal Resources, *PROCESSDINGS, Thirty-Ninth Workshop on Geothermal Reservoir Engineering, Stanford University*, Stanford University, California, 2014.
[12] MATHWORKS, MATLAB Script, Free MATLAB Trial, MATLAB.
[13] ANSYS, Fluent, ANSYS Student, ANSYS.

Corresponding Author:
Hong Duc Thong, PhD
Ho Chi Minh City University of Technology
Email: hongducthong@hcmut.edu.vn; ducthonghong@gmail.com